Polish Journal of Chemical Technology, 19, 3, 61—67, 10.1515/pjct-2017-0050

Enhancement photocatalytic activity of spinel oxide(Co, Ni) $_3O_4$ by combination with carbon nanotubes

Bashaer J. Kahdum[1], Abbas J. Lafta[2*], Amir M. Johdh[1]

[1]*University of Kufa, College of Science- Department of Chemistry, Iraq*
[2]*University of Babylon, College of Science-Department of Chemistry, Iraq*
[*]*Corresponding author: e-mail: abbaslafta2009@yahoo.com*

In this study, some types of composites consisting of multi-walled carbon nanotubes (MWCNTs) and spinel oxide (Co, Ni) $_3O_4$ were synthesized by simple evaporation method. These composites were characterized by UV–Vis diffuse reflectance spectroscopy, X-rays diffraction(XRD), Scanning electron microscopy (SEM) and specific surface area(S_{BET}). The photocatalytic activity of the prepared composites was investigated by the following removal of Bismarck brown G (BBG) dye from its aqueous solutions. The obtained results showed that using MWCNTs in combination with spinel oxide to produced composites (spinel/MWCNTs) which succeeded in increasing the activity of spinel oxide and exhibited higher photocatalytic activity than spinel oxide alone. Also it was found that, multi-walled carbon nanotubes were successful in increasing the adsorption and improving the activity of photocatalytic degradation of Bismarck brown G dye(BBG). The obtained results showed that spinel/MWCNTs was more active in dye removal in comparison with each of spinel oxide and MWCNTs alone under the same reaction conditions. Also band gap energies for the prepared composites showed lower values in comparison with neat spinel. This point represents a promising observation as these composites can be excited using a lower energy radiation sources.

Keywords: MWCNT, spinel oxide, spinel/CNTs composite, Bismarck brown G degradation, photocatalytic activity.

INTRODUCTION

Dyes have long been used in different types of industries such as dyeing, textiles, paper, plastics, leather and cosmetics[1]. Color stuff discharged from these industries pose hazards and has an environmental impact[2]. The presences of dyes in water are causing some problems such as reducing oxygen levels in water; interfering with penetration of sunlight into waters; retarding photosynthesis and interfering with gas solubility in water bodies[3]. Among different types of textile synthetic dyes Azo dyes are important type, and these dyes can be divided according to the presence of azo bonds (–N=N–) in the molecule. These include mono azo, diazo, and triazo[4]. Azo dyes resist the effect of oxidation agents and light, thus they cannot be completely treated by conventional methods of anaerobic digestion[5]. It is necessary to find an effective method for the treatment of these dyes. The degradation of the synthetic dyes can be achieved in the presence of photocatalysts such as zinc oxide, cobalt oxide (Co_3O_4), nickel oxide (Ni_3O_4) and titanium dioxide. These photocatalysts can be used effectively in treatment of pollution of water with these dyes[6].

Among different methods that can be applied in dye treatment, photocatalytic degradation methods seem to be an interesting alternative method that can be used effectively in the removal of these dyes from textile effluents. According to this method, semiconductors photocatalysts play an important role in dyes removal from their wastewaters[7–10].

These photocatalysts have large surface area, inert, relatively cheap, thermally stable, easy to prepare, and they are easy to be recycled for further usage. Due to all of these excellent properties, they can be widely used in heterogeneous catalyst preparation[11, 12]. Generally, cobalt oxide (Co_3O_4) has important catalytic properties which enable it to be used for many environmental applications. Cobalt oxide is an important catalyst that can be used effectively for oxidation of many types of volatile organic compounds. Nickel oxide has a distorted structure due to the presence of excess oxygen that make holes between the neighboring ions of Ni^{2+} ions. This leads to oxidation of Ni^{2+} to Ni^{3+}, it's believed that this process is responsible for the oxide color[13, 14]. Generally, the above oxides can be used singly, coupled as well as a supported co-catalyst as a heterogeneous photocatalyst in the heterogeneous photocatalytic systems. One important application of these systems is their utilization in photocatalytic degradation of environmental pollutants. Currently, many efforts were directed towards modifying the electronic band of semiconductors such as metal/nonmetal doping, photosensitization with dyes and coupling with secondary semiconductors. The common materials which used to make coupling effect between adsorption[15, 16] and photocatalysis are the carbonaceous species such as mesoporous carbons[17], carbon nanofibers[18], graphenes[19, 20] and Carbon Nanotubes[21–28]. Carbon nanotubes can be classified to single-walled carbon nanotubes (SWCNTs) and multi-walled carbon nanotubes (MWCNTs). Electrical properties of CNTs are mainly dependent on the chiral angle and according to this value CNTs exhibit either metallic or semiconducting properties[29–35].

The present study involves the synthesis of composites of MWCNTs/spinel at different ratios (0.5, 1, 5, 10% MWCNTs/$(Co, Ni)_3O_4$. The activity of both spinel and composites were investigated by removal of BBG from simulated textile wastewaters over a suspension of MWCNTs/spinel.

MATERIAL AND METHODS

Material and chemicals

MWCNTs that were used in this study purchased from Aldrich with a purity of 95% and carbon nanotubes

with mode diameter of 5.5 nm. Cobalt nitrate hexahydrate $Co(NO_3)_2 \cdot 6H_2O$, nickel nitrate hexahydrate $Ni(NO_3)_2 \cdot 6H_2O$ were obtained from the BDH Company with Purity 97.9, 99.9%, respectively. Sodium carbonate anhydrous Na_2CO_3 obtained from GmbH with Purity 99.9%, HCl and NaOH were obtained from BDH Company. The used dye in this study was Bismarck brown G (BBG) with a molecular formula ($C_{21}H_{24}N_8 \cdot 2HCl$) and it was obtained from Al-Hilla Textile Factory(Iraq).

Catalyst synthesis

The supported co-catalyst was prepared by co-precipitation method. According to this method, 50% of $Co(NO_3)_2 \cdot 6H_2O$, 50% of $Ni(NO_3)_2 \cdot 6H_2O$ were weighed accurately and dissolved in 400 ml of distilled water with a continuous stirring at room temperature under normal atmospheric conditions. The pH of the resultant mixture was adjusted using a digital pH meter to maintain pH at a required value. To this mixture, Na_2CO_3 (1M) was added dropwise as a precipitating agent and the solution was kept at a temperature around (70–75°C). Then the value of the pH of the produced mixture was kept around 9.0. The resultant mixture was left for 2 hours at the same temperature with continuous stirring under air conditions. The obtained mixture was filtered of with a Buchner filtration flask with a vacuum pump. The obtained solid was dried in an oven overnight at approximately 120°C. Then this material was calcined at 500°C at a heating rate of 10°C/min for 4 hrs. under normal air atmosphere[36].

Preparation of binary composites

Before synthesizing the binary composites, MWCNTs were activated by treating with a mixture of acid HNO_3/ H_2SO_4 (1/3) with an ultrasonic water bath for 7 hours[37]. This mixture was used as a strong oxidation reagent to introduce some functional groups on the surface of CNTs. Then 1.0 g of (Co, Ni) $_3O_4$ was suspended in 100 ml of distilled water for 30 minutes using an ultrasonic water bath. Then a desired weight of MWCNTs was added to suspension of (Co, Ni) $_3O_4$ using ultrasonic water bath. Then the obtained mixture was filtered off using a vacuum evaporator (Rota vapor re121 BUSHI 461 water Bath) at 45°C. The obtained composite was dried overnight in an oven at 110°C to avoid any physicochemical changes in the carbon materials that occur in higher temperatures in the presence of oxygen.

Activity of spinel and the composite of spinel/MWCNTs

The photocatalytic activity of pristine, (Co, Ni) $_3O_4$ and CNTs/ (Co, Ni) $_3O_4$ at different ratios was investigated by removing of BBG dye from simulated textile wastewaters. The catalysts (120 mg) were suspended in 100 ml of 50 ppm Bismarck Brown G solutions to a glass vessel. Irradiation of reaction mixture was carried out with UV light with light intensities 1.3 mW/cm^2.The reaction mixture was adjusted to a constant temperature at 23°C. Prior to irradiation, the suspension was magnetically stirred in the dark to ensure the establishment of an adsorption/ desorption equilibrium. Then the reaction was initiated by flashing UV radiation from middle pressure mercury lamp. Then periodically, 2 ml of reaction mixture was withdrawn at each 10 minutes for a period of one hour of reaction duration. These samples were collected and centrifuged carefully to remove any fine particles that may remain in the supernatant liquid. Then the absorbance's were recorded at 468 nm using UV-Visible spectrophotometer (Shimadzu 1100A).

Study effect of duration time and catalyst dosages on dye removal

In order to investigate the effect of duration time of reaction and the dosage of the used catalyst on the efficiency of dye removal. A series of experiments were performed using 100 ml of 50 ppm of BBG dye solution with continuous stirring for one hour using a graduated catalyst masses (5, 10, 15, 20, 25 and 30 mg). The absorbance of each sample was measured at λ max = 468 nm.

RESULTS AND DISCUSSION

Characterization of MWCNTs/ (Co, Ni) $_3O_4$

The UV-Vis reflectance spectra of the prepared composites were measured at room temperature in air on Shimadzu 1100A UV-Vis spectrophotometer equipped over the range from 300–600 nm. BaSO4 was used as a standard reflectance to measure UV-Vis diffuse reflectance spectra. The X-ray diffraction patterns of the prepared materials were measured on a Phillips X-ray diffraction with CuKα radiation (1.542 A, 40 KV, 30 MA), in the 2θ range, 10–80 degrees. XRD 6000, Shimadzu, Japan. Surface area measurements of (Co, Ni) $_3O_4$ powders were performed by the Bruner-Emmett-Teller (BET) method, performed on a 060 and Gemini BET machine. According to this technique, 0.05 g of each sample was dried with flushing N_2 gas to remove pre-adsorbed gases in the sample. Then BET specific surface areas of the prepared co-catalysts were performed via adsorption of nitrogen at –196°C.

Figure 1 shows the UV-Vis diffuse reflectance spectra of spinel and CNT/spinel composites. From the obtained results it can be seen that, there is a red shift in absorbance for composites in UV- light region for composited in comparison with the spinel. This probably due to due to intrinsic property of CNTs, inhomogeneous mixing between (Co, Ni) $_3O_4$ and CNTs which can act as an excellent carrier of electrons[38].

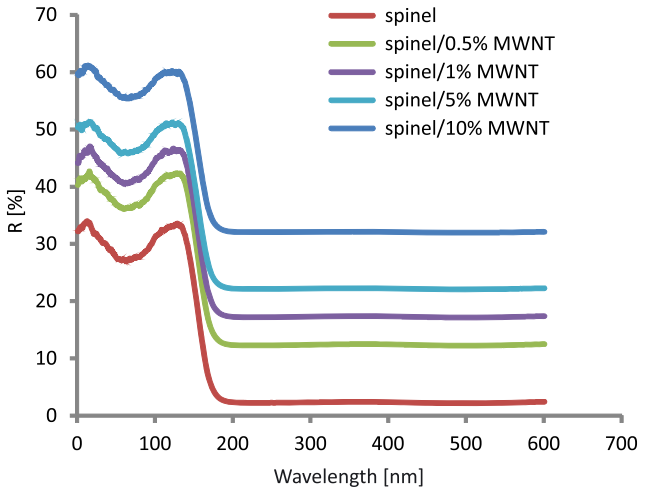

Figure 1. Band gap energy for spinel and composites of spinel/ CNTs at different ratios

The XRD patterns were used to investigate crystal structure of the spinel and composites. Agglomerations were estimated by line broadening using Debye–Scherer equation as shown in the following equation[39]:

$$D = K \lambda / \beta \cos\theta$$

where as, D is the average crystallite size, λ is the X-ray wavelength in nanometer (nm) and it is equal to (0.15405 nm), β is the peak width of the diffraction peak profile at half maximum height resulting from small crystallite size in radians and K is a constant related to crystallite shape mostly equal to 0.9 for homogeneous shape and (0.89) for heterogeneous shape. Figure 2 shows the characteristic peaks of MWCNTs which appeared at $2\theta = 25.9^{o}$ and 43.2^{o} due to diffraction changed from C (100) and C (002) planes of the carbon nanotubes[40].

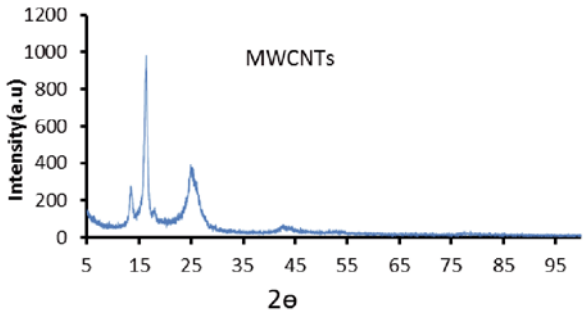

Figure 2. XRD patterns for MWCNTs

From the obtained XRD patterns for spinel as shown in Figure 3, the peaks at 37.26°, 43.29°, 62.88° and 75.41° are corresponded to (111), (200), (220) and (311) planes respectively. These are the characteristic reflection peaks for the nickel oxide[41]. The peaks at 36.86°, 38.57°, 44.82°, 55.69°, 59.38°, 65.26° and 74.12° are corresponded to the (220), (311), (222), (400), (422), (511), (440) and (620) planes respectively[41]. These are the characteristic reflection for the cobalt oxide[41].

To form NiO-CoO solid solution a mixture of $Ni(NO_3)_2$ and $Co(NO_3)_2$ was calcined in air at 500°C. For the entire range of Ni/Co molar ratio from 50:50. The positions and relative intensities of the main XRD peaks of the samples are consisted of NiO-CoO having the same structure as NiO and CoO. The XRD patterns of the spinel and spinel/MWCNTs composites prepared with different weight ratios of MWCNTs are shown in Figure 4. The identified peaks of MWCNTs corresponded to the (100) and (200) reflection planes as shown in Figure 4. XRD patterns of the spinel/MWCNTs composite catalysts are very similar to that of spinel alone. Catalysts crystallite was determined by the diffraction broadening of the reflection plane of the spinel ($2\theta = 18.94^{o}$, 31.03^{o}, 36.78^{o}, 43.18^{o}, 59.04^{o}, 62.12^{o}, 65.06^{o}, 75.2^{o}). From these observations there is no interference from CNTs using Scherer·s equation. The crystallite size of the composite catalysts decreases gradually with the increasing in the ratios of MWCNTs, for 0.5 to 10% MWCNTs. The peaks become more intense and wider with increase the ration of MWCNTs in the composite and this means that particle size was reduced upon composition of these materials[42, 43]. This observation can be attributed to the relatively high specific surface area of CNTs which leads to increase of the surface area of the composites with reduction in the average particle size in comparison with the neat spinel. For pristine and modifying spinel, the first peak disappears in binary composite. The diffraction peaks of MWCNTs were not observed clearly. This probably due to embedding composites peak by much more intense peak for the large ratio of spinel(Co, Ni) $_3O_4$ or the low loading amount of the carbon nanotube[43].

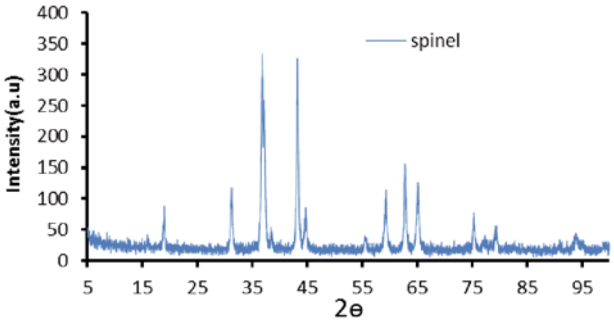

Figure 3. XRD patterns for spinel (Co, Ni) $_3O_4$ oxide

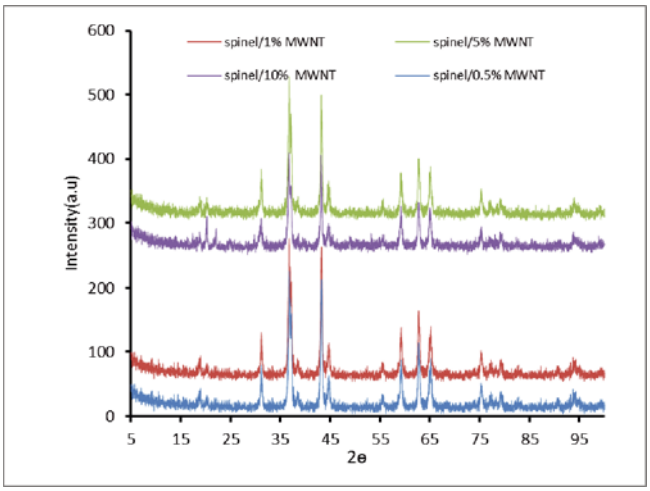

Figure 4. XRD patterns for pristine and modify spinel (Co, Ni) $_3O_4$ with MWCNTs

Scanning electron microscopy (SEM) was used to study surface morphology of both spinel and composites and the obtained results are presented in Figures 5 and 6. From these images the average particle size for spinel was ranged from (27–64) nm as shown in Figure 5. SEM images of the composites are presented in Figure 6, and from these images it is found that CNTs are not found in composites with low ratio of CNTs (0.5% and 1%) and this probably due to embedding of CNTs with spinel matrix. At higher ratio of CNTs within composites (5% and 10%) CNTs can be seen within the matrix of spinel.

The results of specific surface area and band gap energy for both spinel and the different composites are listed in Table 1. From these results it is clear that, addition of MWCNTs to spinel lead to increase specific surface area. This can be attributed to the high distribution of MWCNTs in the matrix of spinel and strong interactions between composites materials. Beside that band gap energy of the obtained composites was decreased with increase the ratio of CNTs in the composites.

Due to intrinsic structure of CNTs it is having high specific surface area with relatively small band gap energy in comparison with neat spinel oxide. So that the obtained composites are expected to show lower band

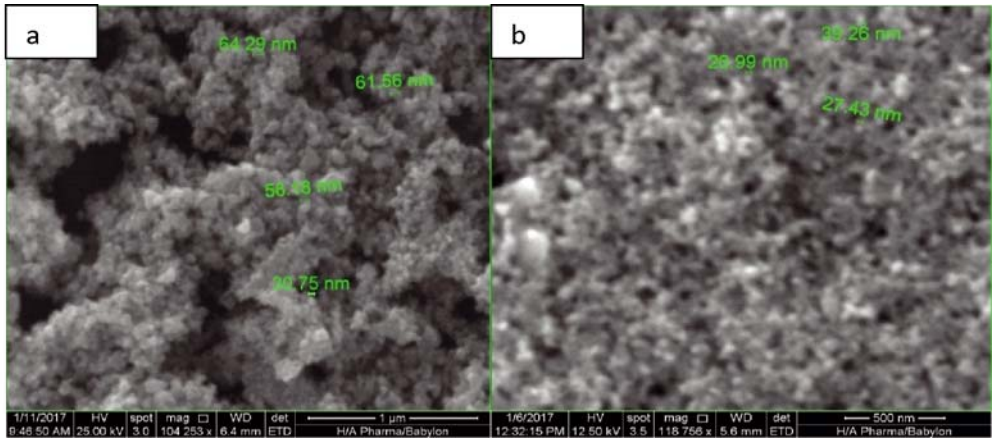

Figure 5. SEM images of the spinel oxide (a and b)

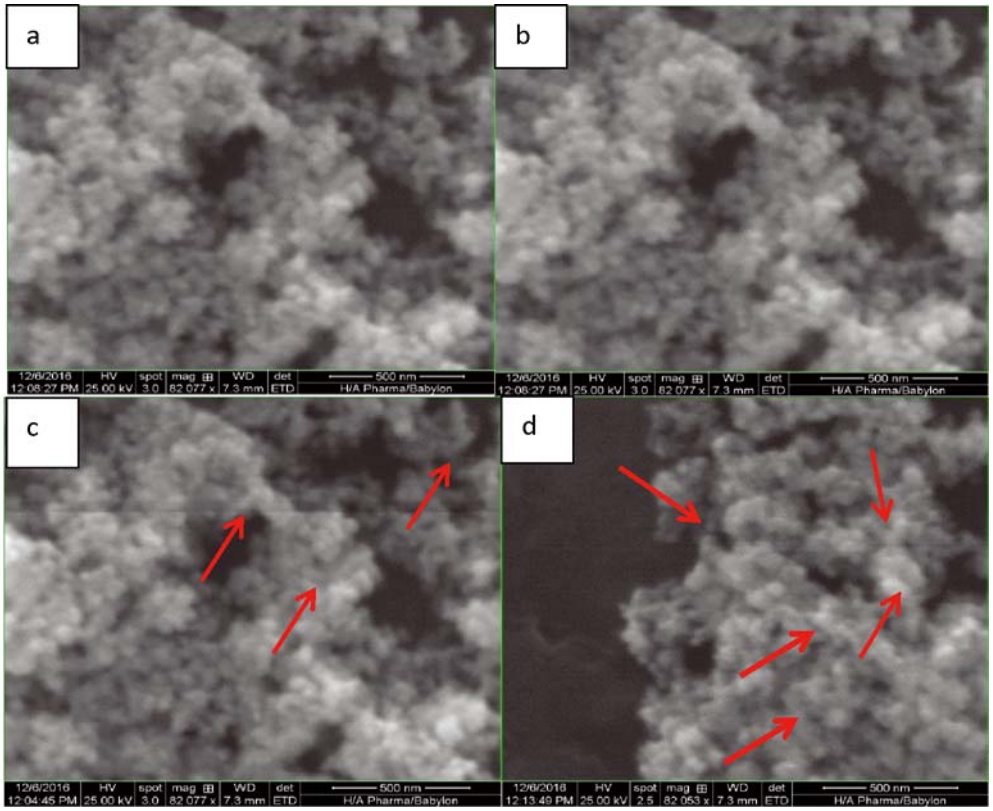

Figure 6. SEM images for the composites (0. 5% (a), 1% (b), 5% (c), and 10% (d))

gap energy and this probably arises from contribution of CNTs in reduction of band gap energy of the produced composites. Consequently as the ratio of CNTs in the prepared composites was increased this effect becomes more effective and leads to reduce band gap energies of the composites with higher ratios of CNTs[44].

Effect of MWCNTs ratio on adsorption of BBG dye over composites

The results of adsorption of BBG dye over each spinel (Co, Ni) $_3O_4$ and different binary composites are shown in Figure 7. The obtained results showed that there was enhancement on dye adsorption over the composites in comparison with that for spinel alone under the same applied conditions. Efficiency of dye removal was increased as follows, spinel/10%MWCNTs > spinel/5%MWCNTs> spinel/1%MWCNTs> spinel/0.5%MWCNTs> spinel. This can be attributed to the role of CNTs in increasing the adsorption capacity of the composite as it has high surface area with high porosity[44].

Table 1. Band gap energy and specific surface area of spinel and composites of MWCNTs/Spinel

Sample	Band gap energy [eV]	BET [m^2/g]
Spinel alone	3.170	127.30
Spinel/0.5%MWCNTs	3.024	129.10
Spinel/1%MWCNTs	2.883	134.26
Spinel/5%MWCNTs	2.818	132.30
Spinel/10%MWCNTs	2.480	151.80

Photocatalytic removal of BBG dye over spinel and composites

Photocatalytic removal of BBG over pristine spinel and the prepared composites are shown in Figure 8. From these results it can be seen that, there was enhancement on the activity of dye removal over composites in comparison with spinel alone. Also it was found that there was enhancement in dye removal over composites as the ratio of CNTs of the composites was increased. Generally, dye removal was increased with increase of

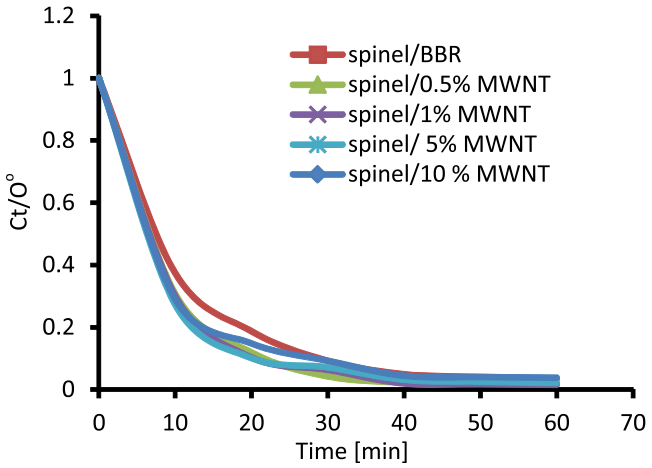

Figure 7. Dark reaction for spinel, spinel/0.5, 1.5 ,10% MWCNTs with, 50 ppm BBG at 298 K

CNTs on the composites due to enhance of adsorption ability. This is an essential step in photocatalytic reaction on heterogeneous photocatalysis processes. In this type of reaction, the first step is the adsorption of reacting species on the active sites of the catalyst surface. Then these adsorbed species can react with active surface radicals that are produced due to interaction of hydroxyl radicals and super oxide radicals with conduction band electrons and valence band holes that are produced when irradiation of the catalyst particle with a light of a proper energy[44, 45]. From mechanistic view, photodegradation dye removal over photocatalyst under irradiation with UV light follows the pseudo first-order kinetics with respect to the concentration of dyestuff in the bulk solution (C):

$-dC/dt = K_{app}C$

By Integration of this equation and by using the same restriction of $C = C_o$ at time = 0, and C_o being the initial concentration in the bulk solution before starting the light reaction, thus the equation becomes:

$Ln_{Co}/C = K_{app}t$

where K_{app} is the apparent reaction rate constant. A plot of ln (C_o/C) versus t for BBG degradation with different composite of MWCNTs/ spinel photocatalysts is shown in Figure 8. The value of K_{app} can be obtained directly from the slope of the respective linear curves in the Figure 9. Comparing the K_{app} for the photodegradation of BBG dye with spinel and the many types of composites.

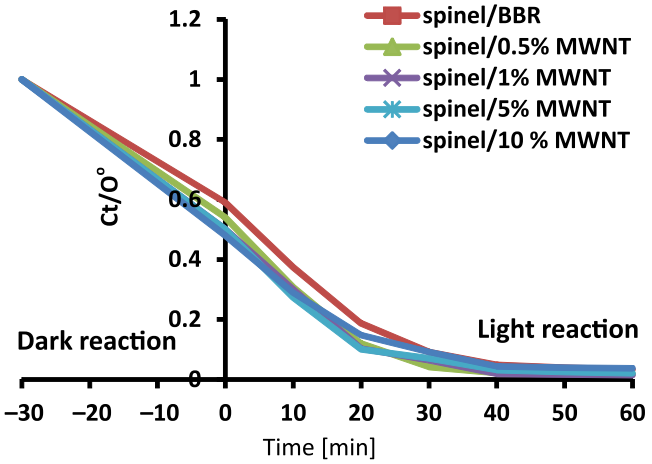

Figure 8. Photocatalytic removal of BBG dye 50 ppm using (20 mg) of spinel, and (0.5, 1.5, 10%)MWCNTs/ spinel at 298 K under O_2 gas and light intensity of 1.3 m W/cm^2

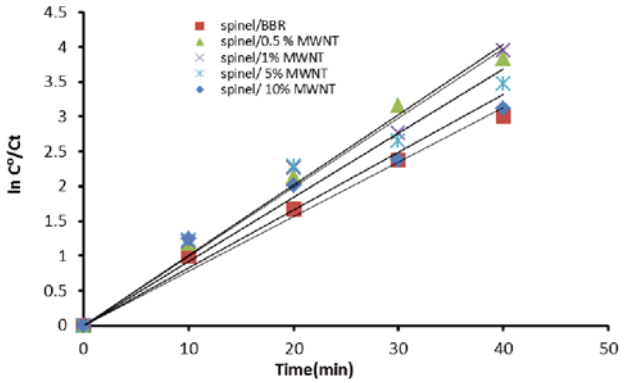

Figure 9. Plot of changes in ln(Co/Ct) with adsorption time for spinel and (0.5, 1.5, 10%)MWCNTs/ spinel using 50 ppm BBG at 298K in presence of O_2 gas and light intensity of 1.3 m W/cm^2

Rate = k_{app} (spinel/ CNT)/ k_{app} (spinel)

whereas, k_{app} (spinel/ MWCNTs), k_{app} (spinel) refer to the apparent rate constant for decolorization in existence of composite and spinel respectively[45]. The presence of MWCNTs can cause increasing in decolorization rate and that can be attributed to increase the ability of adsorption for spinel in existing of MWCNTs in composite[45].

Under UV illumination electrons are excited from valances band to the conduction band of the spinel. This leads to forming positive hole h^+ in valance band and negative charge e^- in conduction band. However, these charges can recombine quickly which leads to loss excitation energy via recombination reaction. This process normally occurs in case of use naked phtocatalyst and leads to reduce the efficiency of the photocatalytic reaction[46]. When using composites of spinel/ MWCNTs, CNTs are attached to the surfaces of spinel and in this case exited electrons in conduction band of spinel transfer to the surfaces of MWCNTs. This can lead for separation and prevent or at least reduce recombination process[46].

This effect can lead to increase the live time for positive hole and then contribution in formation of OH surface radicals in high concentration and the exited electron can react with O_2 gas to form superoxide O_2– radicals. Addition of small quantities MWCNTs to the semiconductors can cause changes on the conductivity , this can improve the conductivity of the spinel[47, 48]. Also adding CNTs into the spinel can reduce the agglomerations of spinel in binary composites which leads to appear more active site. In composites of spinel/CNTS, e^-/h^+ would diffuse into two opposite directions, e^- on the surfaces of CNTs more ability to accept the electrons, then spinel. The h^+ or the positive charge remain without electron for more time (equation 1). The new active distribution of charge start to produce free radical. The first O_2 forming when the e^- react with O_2 (equation 2). The second equation represents reacting of hydroxide ion with h^+ which produces OH (equation 3).

$$\text{spinel/CNT} + h\upsilon \rightarrow \text{spinel}^{\,h+VB}/\ \text{CNT}^{e\text{-}CB} \quad (1)$$

$$\text{spinel}^{\,h+VB}/\ \text{CNT}^{e\text{-}CB} + O_2 \rightarrow O2 + \text{spinel}^{\,h+VB}/\ \text{CNT} \quad (2)$$

$$\text{spinel}^{\,h+VB}/\ \text{CNT} + {}^{-}OH \rightarrow OH + \text{spinel/CNT} \quad (3)$$

CONCLUSIONS

In this work three ratios of MWCNTs were combined with the spinel oxide (Ni, Co) $_3O_4$ to yield spinel/

MWCNTs composites. These materials were prepared This process was performed using simple evaporation method. Form the obtained results in this study it was found that, the composite showed higher ability on dye removal in comparison with the single components. The coupling effect of adsorption/photocatalytic processes which occur between carbon nanotubes (MWCNTs) and spinel oxide is expected to show a remarkable enhancement in the efficiency of BBG dye removal under the applied reaction conditions. Besides that the prepared composites showed higher specific surface areas with lower band gap energies in comparison with single components materials.

LITERATURE CITED

1. Hussein, F.H., Halbus, A.F., Lafta, A.J. & Athab, Z.H. (2015). Preparation and Characterization of Activated Carbon from Iraqi Khestawy Date Palm. J. Chem. 1–8. http://dx.doi.org/10.1155/2015/295748.

2. Falah, H.H., Ahmed, F.H., Hussein, Hassan, A.K. & WIisam, Hussein, A.K. (2010). Photocatalytic Degradation of Bismarck Brown G Using Irradiated ZnO in Aqueous Solutions. E-J. Chem. 7(2), 540–544. http://www.e-journals.net.

3. Garg, V.K., Amita, M., Kumar, R. & Gupta, R. (2004). Basic dye (methylene blue) removal from simulated wastewater by adsorption using Indian rosewood sawdust: a timber industry waste. Dyes Pigm. 63(3), 243–250. http://dx.doi.org/10.1016/j.dyepig.2004.03.005.

4. Hussein, F.H. (2013). Chemical Properties of Treated Textile Dyeing Wastewater. Asian J. Chem. 25(16), 9393–9400. DOI: 10.14233/ajchem.2013.15909A.

5. Garg, V.K., Amita, M., Kumar, R. & Gupta, R. (2004). Basic dye (methylene blue) removal from simulated wastewater by adsorption using Indian rosewood sawdust: a timber industry waste. Dyes Pigments. 63(3), 243–250. http://dx.doi.org/10.1016/j.dyepig.2004.03.005.

6. Abbas, J.A., Salih, H.K. & Falah, H.H. (2008). Photocatalytic degradation of textile Dyeing wastewater using titanium dioxide and zinc oxide. E-J. Chem. 5(2), 219–223. http://www.e-journals.net.

7. Robinson, T., McMullan, G., Marchant, R. & Nigam, P. (2001). Remediation of dyes in textile effl uent: a critical review on current treatment technologies with a proposed alternative. Biores. Technol. 77(3), 247–255. DOI: 10.1016/S0960-8524(00)00080-8.

8. Zamora, P., Kunz, A., Moraes, S., Pelegrini, R., Molerio, P., Reyes, J. & Duran, N. (1999). Chemosphere. Degradation of Reactive Dyes I. A Comparative Study of Ozonation, Enzymatic and Photochemical Processes. Chemosphere 38(4), 835–852. DOI: 10.1016/S0045-6535(98)00227-6.

9. Ladakowicz, L., Solecka, M. & Zylla, R. (2001). Biodegradation,decolourisation and detoxifi cation of textile wastewater enhanced by advanced oxidation processes, J. Biotech. 89(2–3), 175–184. DOI: 10.1016/S0168-1656(01)00296-6.

10. Georgiou, D., Melidis, P., Aivasidis, A. & Gimouhopoulos, K. (2002). Degradation of azo-reacti ve dyes by ultraviolet radiation in the presence of hydrogen peroxide. Dyes Pigm. 52, 69–78. DOI: 10.1016/S0143-7208(01)00078-X.

11. Farrauto, R. & Bartholomew, C. (1997). Fundamentals of Industrial Catalytic Processes, Chapman & Hall, Kluwer Academic Publishers, London.

12. Pourbaix, M. (1974). Atlas of Electrochemical Equilibrium,Pergamum Press, New York, Translated from French by J.A. Franklin**,** USA.

13. Pal, J. & Chauhan, P. (2010). Study of physical properties of cobalt oxide (Co3O4) nanocrystals. Mater. Character. 61(5), 575–579. DOI: 10.1016/j.matchar.2010.02.017.

14. Sujia, T.T., Hamagamia, T., Kawamurab, T., Yamakia, J. & Masaharu, T. (2005). Laser ablation of cobalt and cobalt oxides in liquids: infl uence of solvent on composition of prepared nanoparticles. Japan Appl. Surf. Sci. 243(30), 214–219. DOI: 10.1016/j.apsusc.2004.09.065.

15. Alkaim, A.F., Sadik, Z., Mahdi, D.K., Alshrefi, S.M., Al-Sammarraie, A.M., Alamgir, F.M., Singh, P.M. & Aljeboree, A.M. (2015). Preparation, structure and adsorption properties of synthesized multiwall carbon nanotubes for highly effective removal of maxilon blue dye. Korean J. Chem. Eng. 32(12), 2456–2462. DOI: 10.1007/s11814-015-0078-y.

16. Aljebori, A.M. & Alshirifi, A.N. (2012). Effect of Different Parameters on the Adsorption of Textile Dye Maxilon Blue GRL from Aqueous Solution by Using White Marble. Asian J. Chem. 24, 5813–5816. www.asianjournalofchemistry.co.in.

17. Ren, W., Ai, Z., Jia, F., Zhang, L., Fan, X. & Zou, Z. (2007). Low temperature preparation and visible light photocatalytic activity of mesoporous carbon-doped crystalline TiO2. Appl. Catal. B: Environmental 69(3–4), 138–144. http://dx.doi.org/10.1016/j.apcatb.2006.06.015.

18. Yang, Z., Du, G., Meng, Q., Guo, Z., Yu, X., Chen, Z., Guo, T. & Zeng, R. (2012). Synthesis of uniform TiO2@carbon composite nanofibers as anode for lithium ion batteries with enhanced electrochemical performance. J. Mater. Chem. 22, 5848–5854. DOI: 10.1039/c2jm14852h.

19. He, H.Y., Fei, J. & Lu, J. (2015). High photocatalytic and photo-Fenton-like activities of ZnO-reduced graphene oxide nanocomposites in the degradation of malachite green in water. Micro and Nano Lett. 10(8), 389–394. DOI: 10.1049/mnl.2014.0551.

20. Shen, J., Yan, B., Shi, M. & Mingxin, Y. (2011). One step hydrothermal synthesis of TiO2-reduced graphene oxide sheets. J. Mater. Chem. 21(10), 3415–3421. DOI: 10.1039/C0JM03542D.

21. Abdulrazzak, F.H. (2016). Enhance photocatalytic Activity of TiO_2 by Carbon Nanotubes. Inter. J. Chem. Tech. Res. 9(3), 431–443. www.sphinxsai.com

22. Salam, M.A., El-Shishtawy & Obaid, R.M.A.Y. (2014). Synthesis of magnetic multi-walled carbon nanotubes/magnetite/chitin magnetic nanocomposite for the removal of Rose Bengal from real and model solution. J. Ind. Enginee. Chem. 20(5), 3559–3567. DOI: 10.1016/j.jiec.2013.12.049.

23. Gupta, V.K., Agarwal, S. & Saleh, T.A. (2011). Synthesis and characterization of alumina-coated carbon nanotubes and their application for lead removal. J. Hazard. Mater. 185(1), 17–23. DOI:10.1016/j.jhazmat.2010.08.053.

24. Dervishi, E., Watanabe, F., Xu, Y., Saini, V., Biris, A.R. & Biris, A.S. (2009). Thermally controlled synthesis of single-wall carbon nanotubes with selective diameters. J. Mat. Chem. 19(19), 3004–3012. DOI: 10.1039/b822469b.

25. Yao, Y., Li, G., Ciston, S., Lueptow, R.M. & Gray, K.A. (2008). Photoreactive TiO2/Carbon Nanotube Composites: Synthesis and Reactivity. Environ. Sci. Technol. 42(13), 4952–4957. DOI: 10.1021/es800191n.

26. Manafi, S., Nadali, H. & Irani, H.R. (2008). Low temperature synthesis of multi-walled carbon nanotubes via a sonochemical/hydrothermal method. Mater. Lett. 62(26), 4175–4176. http://dx.doi.org/10.1016/j.matlet.2008.05.072.

27. Sun, Z., Zhang, X., Liu, Z., Han, B. & An, G. (2006). Synthesis of ZrO_2-Carbon Nanotube Composites and Their Application as Chemiluminescent Sensor Material for Ethanol. J. Phys. Chem. B. 110(27), 13410–13414. DOI: 10.1021/jp0616359.

28. Hussein, F.H., Obies, M.H. & Abed, A.A. (2010). Photocatalytic Decolorization ofBismarck Brown R by Suspension of Titanium Dioxide. Int. J. Chem. Sci. 8(4), 2736–2746. https://www.researchgate.net/publication/299595106.

29. Opalińska, A., Malka, I., Dzwolak, W., Chudobe, T., Presz, A., Lojkowski, W. & Ron, N. (2015). Size-dependent density of zirconia nanoparticles. Beil. J. Nanotech. 2015; 6: 27–35. DOI: 10.3762/bjnano.6.4.

30. Zhenyu, S., Xinrong, Z., Zhimin, L., Buxing, H. & Guimin, A. (2006). Synthesis of ZrO2−Carbon Nanotube Composites and Their Application as Chemiluminescent Sensor Material for Ethanol. J. Phys. Chem. B 110(27), 13410–13414. DOI: 10.1021/jp0616359.

31. Karam, F.F., Kadhim, M.I. & Alkaim, A.F. (2015). Optimal conditions for synthesis of 1, 4- naphthaquinone by photocatalytic oxidation of naphthalene in closed system reactor, Int. J. Chem. Sci. 13, 650–660. www.sadgurupublications.com.

32. Alkaim, A.F., Dillert, R. & Bahnemann, D.W. (2015). Effect of polar and movable (OH or NH2groups) on the photocatalytic H2 production of alkyl-alkanolamine: a comparative study. Environ. Technol. 36(17), 2190–2197. DOI: 10.1080/09593330.2015.1024757.

33. Šíma, J. & Hasal, P. (2013). Photocatalytic Degradation of Textile Dyes in aTiO2/UV System. Chem. Enginee. Trans. 32, 80–84. DOI: 10.3303/CET1332014.

34. Kandiel, T.A., Robben, L., Alkaim, A. & Bahnemann, D. (2013). Brookite versus anatase TiO2 photocatalysts: phase transformations and photocatalytic activities. Photochem. Photobiol. Sci. 12(4), 602–609. DOI: 10.1039/c2pp25217a.

35. Zhen, L., Shan, C., & Yiming, X. (2014). Brookite vs Anatase TiO2 in the Photocatalytic Activity for Organic Degradation in Water. ACS Catal. 4(9), 3273–3280. DOI: 10.1021/cs500785z.

36. Mohammad, E.J., Lafta, A.J., & Kahdim, S.H. (2016). Photocatalytic removal of reactive yellow 145 dye from simulated textile wastewaters over supported (Co, Ni)3O4/Al2O3 co-catalyst. Pol. J. Chem. Technol 18(3),1–8. DOI: 10.15P1o5l/.p jJc. t-C2h0e1m6-.0 0T4ec1h.

37. Wepasnick, K.A., Smith, B.A., Schrote, K.E., Wilson, H.K., Diegelmann, S.R. & Fairbrother, D.H. (2011). Surface and structural characterization of multi-walled carbon nanotubes following different oxidative treatments. Carbon. 49(1), 24–36. DOI: 10.1016/j.carbon.2010.08.034.

38. Wang, W., Serp, P., Kalck, P. & Faria, J.L. (2005). Visible light Photodegradation of Phenol on MWNT-TiO2 Composite Catalysts Prepared by a Modified Sol-gel Method. J. Molec. Catal. A. Chem. 235(1), 194–199. DOI: 10.1016/j.molcata.2005.02.027.

39. Wepasnick, K.A., Smith, B.A. & Fairbrother, D.H. (2011). Surface and structural characterization of multi-walled carbon nanotubes following different oxidative treatments. Carbon 49(1), 24–36. DOI: 10.1016/j.carbon.2010.08.034.

40. Akhavan, O., Azimirad, R., Safa, S. & Larijani, M. (2010). Visible light photo-induced antibacterial activity of CNT-doped TiO2 thin films with various CNT contents. J. Mater. Chem. 20(35), 7386–7392. DOI: 10.1039/C0JM00543F.

41. Sanchai, K. & Hang, H. (2011). Study of NiO-CoO and Co_3O_4-Ni_3O_4 Solid Solutions in Multiphase Ni-Co-O Systems. Ind. Enginee. Chem. Res. 50(4), 2015–2020. DOI: dx.doi.org/10.1021/ie101249r.

42. Xie, Y.,. Heo, S., Yoo, H., Ali, G. & Cho, S. (2010). Synthesis and Photocatalytic Activity of Anatase TiO_2 Nanoparticles-coated Carbon Nanotubes. Nanoscale Res. Lett. 5, 603–607. DOI: 10.1007/s11671-009-9513-5.

43. Liu, G., Yan, X., Chen, Z., Wang, X., Wang, L., Lu, G. & Cheng, H. (2009). Synthesis of rutile–anatase core–shell structured TiO_2 for photocatalysis. J. Mater. Chem. 19, 6590–6596. DOI: 10.1039/B902666E.

44. Matos, J., Laine, J. & Herrmann, J.M. (1998). Synergy effect in the photocatalytic degradation of phenol on a suspended mixture of titania and activated carbon. Appl. Catal. B: Environmental, 18, 281–291. DOI: 10.1007/s11356-014-2832-9.

45. Slimen, H., Lachheb, H., Qourzal, S., Assabbane, A. & Houas, A. (2015). The effect of calcination atmosphere on the structure and photoactivity of TiO_2 synthesized through an unconventional dopingusing activated carbon. J. Environ. Chem. Enginee. 3(2), 922–929. DOI: 10.1016/j.jece.2015.02.017.

46. Chen, W., Fan, Z., Zhang, B., Ma, G., Takanabe, K., Zhang, X. & Lai, Z. (2011). Enhanced visible-light activity of titania via confinement inside carbon nanotubes. J. Am. Chem. Soc. 133(38), 14896–14899. DOI: 10.1021/ja205997x.

47. Vajda, K., Mogyorosi, K., Nemeth, Z., Hernadi, K., Forro, L., Magrez, A. & Dombi, A. (2011). Photocatalytic activity of TiO2/SWCNT and TiO2/MWCNT nano composites with different carbon nanotube content. Phys. Stat. Sol. B. 248(11), 2496–2499. DOI: 10.1002/pssb.201100117.

48. Naseri, M.G., Saion, E.B., Ahangard, H.A., Hashim, M. & Shaari, A.H. (2011). Simple preparation and characterization of nickel ferrite nanocrystals by a thermal treatment method. Powder Technol. 212(1), 80–88. DOI: 10.1016/j.powtec.2011.04.033.